Eurographics Symposium on Parallel Graphics and Visualization (2004)
Dirk Bartz, Bruno Raffin and Han-Wei Shen (Editors)

# Visualization of Seismic Wave Propagation from Recent Damaging Earthquakes in Japan: Dense Array Observations and Parallel Simulations Using the Earth Simulator

T. Furumura[1] and L. Chen [2]

[1] Earthquake Research Institute, University of Tokyo, Japan
[2] Research Organization for Information Sciences and Technology, Japan

**Abstract**

*This paper presents recent developments of large-scale parallel simulation of seismic wave propagation and concurrent visualization of 3D seismic wavefield using the Earth Simulator supercomputer.*
*The developments of high-performance computing facilities and dense networks of strong ground motion instruments in Japan (K-NET and KiK-net) have now made it possible to directly visualize regional seismic wave propagation during large earthquakes. Our group has developed efficient parallel finite difference method (FDM) code for modeling the seismic wavefield, and a 3D visualization technique, both suitable for implementation on the Earth Simulator. Large-scale 3D simulations of seismic wave propagation have been conducted using these techniques to recast strong ground motions during recent damaging earthquakes such as the 2000 Tottori-ken Seibu ($M_J$7.3) earthquake, the 1923 great Kanto earthquake ($M_J$7.9), and the 1855 Ansei Edo (M7) earthquake.*
*Comparison of the simulation results with the dense array observations provides insights into the nature of complex seismic wave propagation through the heterogeneous subsurface structure in Japan. The simulation results are in very good agreement with the observations in terms of the features of the waveform and the regional intensity pattern, indicating that the simulation is already at a suitable level for use in investigating the expected pattern of ground motions for future earthquake scenarios.*

Categories and Subject Descriptors (according to ACM CCS): J.2 [Physical Sciences and Engineering]: Earth and atmospheric sciences

## 1. Introduction

One of our target for strong motion seismologist is to understand the complex seismic wave behavior imposed by heterogeneous in the crust and the upper-mantle structure, and predicting strong ground motion damage expected for future earthquake scenarios.

The complex source rupture process and heterogeneities along the long wave propagation path form an important control on the regional seismic wavefield, particularly for high-frequency seismic waves. Small-scale heterogeneities such as sedimentary basins introduce significant amplification of ground motion leading to large, prolonged ground shaking in these regions. In order to understand the seismic wave behavior imposed by such heterogeneous structures, and to understand the process of strong motion generation during damaging earthquakes, large-scale computer simulations including such small heterogeneities are indispensable.

The recent developments of the Earth Simulator supercomputer (5120 CPUs, 40 TFlops) have made it possible to realize realistic simulations seismic wave propagation on a regional scale. Our group has developed an efficient parallel finite difference method (FDM) code for implementation on the Earth Simulator, along with a suitable volume visualization technique for the 3D wavefield. The results of the computer simulation can be compared with new nation-wide seismic array (K-NET, KiK-net and FREESIA) comprising more than 1,700 stations across Japan (Figure 1). Detailed comparison of computer simulations with observations is expected to provide a direct means of understanding the nature of the complex seismic wavefield.

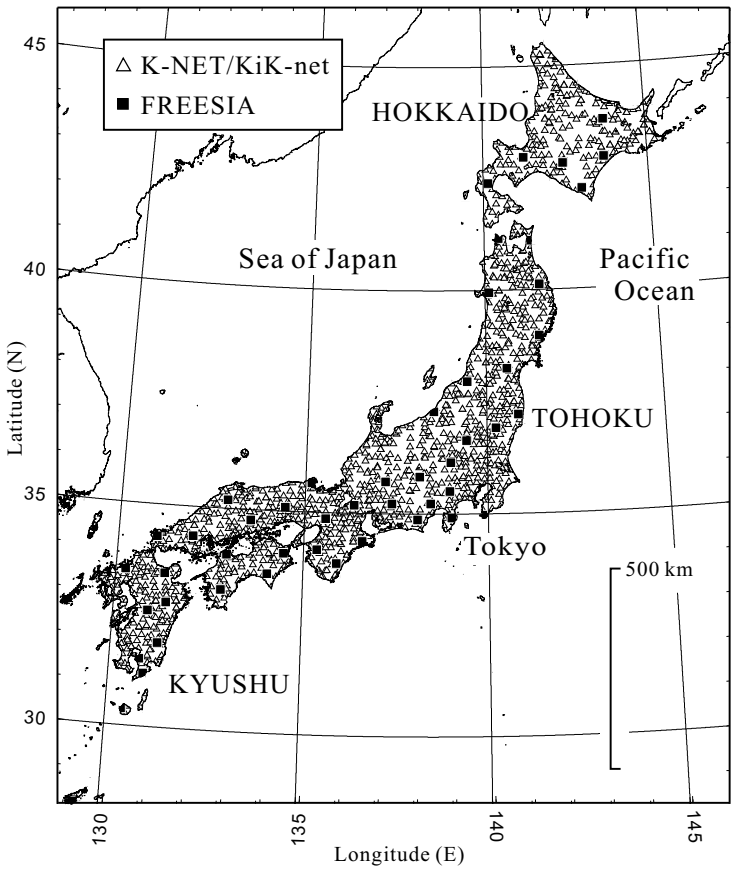


**Figure 1:** *The coverage of strong ground motion instruments (K-NET, KiK-net; triangle) and the FREESIA broadband stations (square) across Japan of over 1700 stations.*

In this paper, the parallel FDM simulation of seismic waves is introduced, and efficient visualization techniques for illustrating the observed and simulated ground motions are presented. Examples for large-scale parallel simulations of seismic wave propagation are shown from comparing the observed and simulated seismic wavefield for recent Tottori-ken Seibu earthquake ($M_J$7.3) in 2000. We also show computer simulation of historical earthquakes such as from the great 1923 Kanto earthquake ($M_J$7.9) and the 1855 Ansei Edo earthquake both caused significant damage in the area around Tokyo metropolitan city.

## 2. Parallel Simulation of Seismic Wave Propagation

The seismic wave propagation in elastic media is expressed by equations of motions in 3D as

$$\rho \ddot{u}_p = \frac{\partial \sigma_{xp}}{\partial x} + \frac{\partial \sigma_{yp}}{\partial y} + \frac{\partial \sigma_{zp}}{\partial z} + f_p, \quad (p = x,y,z), \qquad (1)$$

where $\sigma_{pq}$, $f_p$ and $\rho$ are stress, body force and density, and $\ddot{u}_p$ represents particle acceleration. The stresses in an isotropic elastic medium are given by

$$\sigma_{pq} = \lambda(e_{xx} + e_{yy} + e_{zz})\delta_{pq} + 2\mu e_{pq}, \quad (p,q = x,y,z), \quad (2)$$

with the Lamé's constants $\lambda$ and $\mu$. The strains are defined by

$$e_{pq} = \frac{1}{2}\left(\frac{\partial u_p}{\partial q} + \frac{\partial u_q}{\partial p}\right), \quad (p,q = x,y,z). \qquad (3)$$

The spatial derivatives in Eqs. (1) and (3) can be calculated by the finite difference method (FDM), or more accurately by using the fast Fourier transform (FFT) [RKEH88] [FKT98].

In order to calculate seismic wave propagation accurately to relatively higher frequencies, we use a 16th-order or more higher FDMs rather than based on the spectral scheme employing the FFT, because, the FDM runs very efficiently on the recent vector hardware on the supercomputer as compared with the FFT [FKW02].

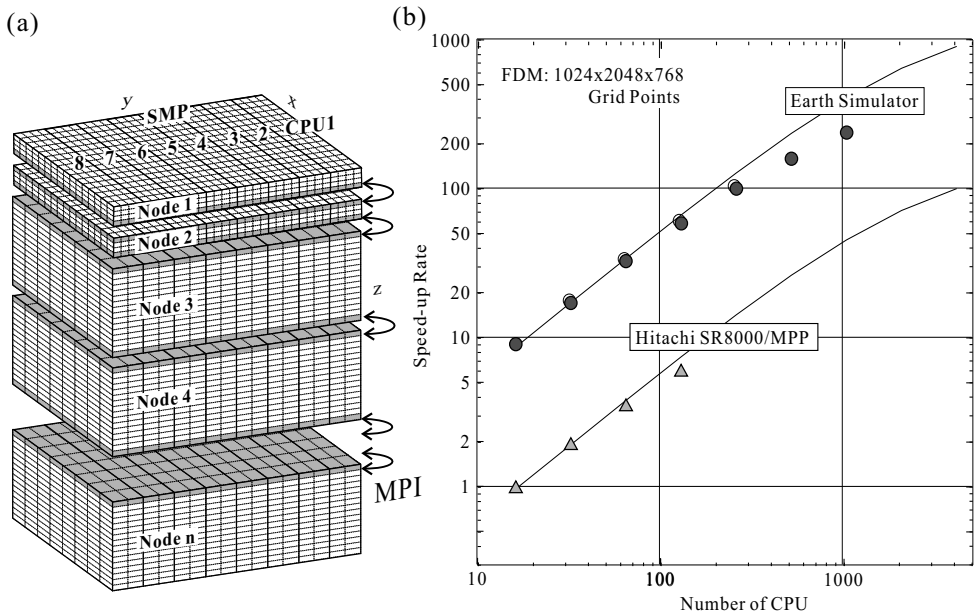


**Figure 2:** *(a)Schematic illustration of the SMP/MPI hybrid parallel algorithm for 3D simulation of seismic wave propagation. (b) Speed-up of the parallel FDM simulation using the Earth Simulator and Hitachi SR8000/MPP as a function of processor numbers. Solid lines are expected theoretical speed-up rate derived from theoretical experiment.*

Parallel simulation of 3D seismic wavefield is achieved by a traditional domain partitioning procedure [FC04]. Each subdomain is assigning to a node of the Earth Simulator for concurrent computing using 8 SMP processors, and the message passing interface (MPI) is used for inter-node parallel computing with exchanging data between neighbor node at each time step [Figure 2(a)]. Such a hybrid parallel approach combining the intra-node SMP parallel algorithm and the inter-node MPI parallel computing achieves very good speed up even using large number of processors on the Earth Simulator [Figure 2(b)] as expected from a theoretical experiment assuming peak processor speed and inter-processor communication speed [FC04].

## 3. Visualization of 3D Seismic Wavefield

We developed a set of efficient visualization techniques for simulated and observed seismic wavefield in order to understand the complex seismic behavior in 3D heterogeneous structure.

### 3.1. Bird's Eye View of Surface Ground Motion

One of our visualization technique used in the present application render 2D seismic wavefield such as for surface ground motions. This approach for visualizing wavefront will be useful to illustrate the propagation of ground motion derived from simulations and observations from dense seismic array [FKK03].

The ground motions are first applied a low-cut filter to remove aliasing effect, and the smoothed ground motion as the gridded data is obtained by interpolation of the filtered waveform using a griding algorithm developed by [SW90]. As the intensity of ground motion manifests on a logarithmic scale of horizontal ground velocity motion, a scalar value of the strength of the ground motion is useful to demonstrate the strength of ground motions. The resulting scalar at each point on the regular mesh, for both observed and simulated ground motions, is then used to render the wavefront using the "height-field" function of the POV-Ray rendering library. In order to highlight the wavefront of larger ground motions and eliminate weak and scattered wavefields (e.g., less than 0.1% of the peak ground motion), an opacity function proportional to the logarithmic amplitude of the ground motion is applied for the rendering.

### 3.2. Concurrent Volume Rendering of Seismic Wavefield

Another visualization technique we use here is for the volume visualization of the simulated 3D seismic wavefield based on the volume rendering technique [Lev88].

As the 3D simulation produces huge data sets in each time step, it is difficult to store all of the simulation results on an external hard disk for post processing. We therefore developed an concurrent parallel volume rendering (PVR) tool for the visualization of 3D wavefield, developed specifically for

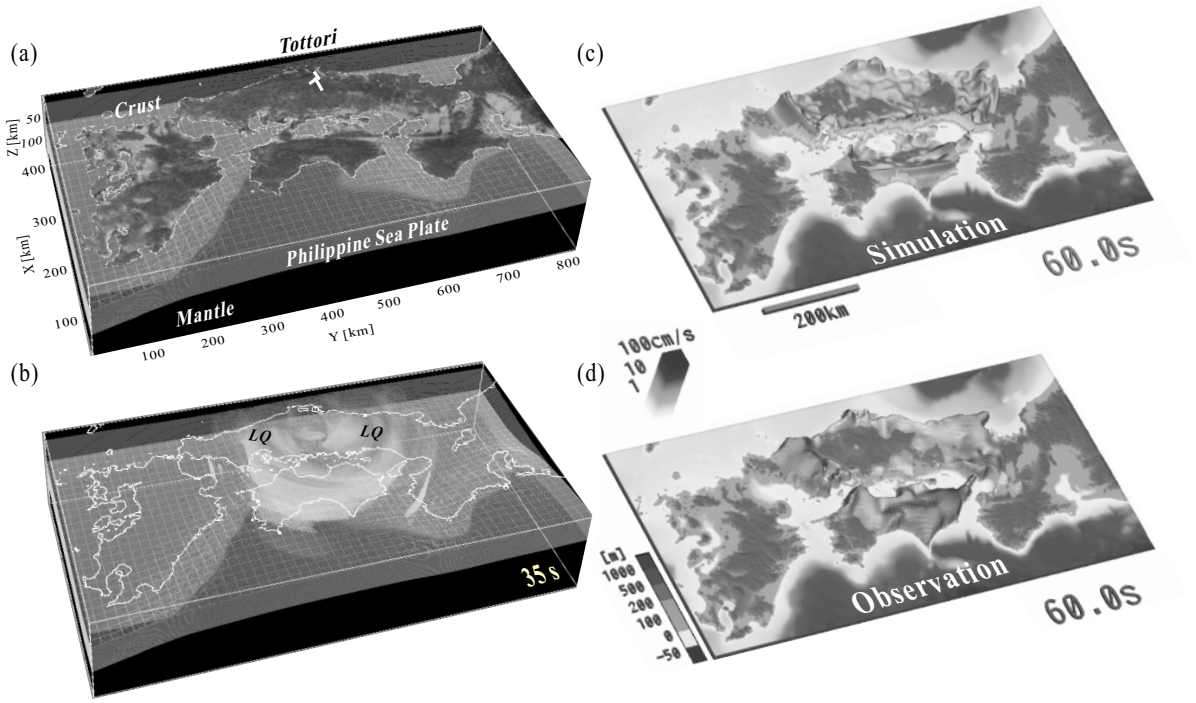


**Figure 3:** *(a) Structural model of western Japan used in the 3D simulation of seismic waves, showing the configuration of crust and upper-mantle structure and the Philippine-sea Plate. Snapshot of (b) seismic wave propagation from the source after 35s from the source initiation, and comparison between the wavefield at 60s for the (c) simulation result with (d) observation by dense seismic array. Color image is shown in last page.*

implementation on the Earth Simulator [CFN03]. This concurrent techniques utilizes data stored on the main memory of the computer, and so the rendering unnecessary to save huge amount of data to an external hard disk or to transfer to another machines over the network.

During the parallel calculation of the seismic waves, the main program of the FDM simulation on each node calls the PVR module at each time step, and the PVR modules generates a frame image from the simulated wavefield at the current time using variables held in the memory.

For treating large dynamic range of the seismic wavefield, the amplitude of the wavefield is compressed by using a logarithm function; A low opacity (large transparency) is assigned to grid points of weak wavefield amplitude, and relatively high opacity is assigned to large wavefield. This highlights the outline of the seismic wavefield clearly, and prevents small, scattered waves from obscuring important features [FC04]. In order to improve the quality of volume rendering, proper opacity transfer functions can be examined. We choose a transfer functions for emphasizing high gradient seismic regions.

Since the graphic processing ability of the Earth Simulator is rather limited, and there is no graphics hardware, such as texture mapping, and alpha-blending, etc. the PVR module make full use of the vector hardware and SMP/MPI hybrid parallel architecture in order to obtain good performance on the visualization. The current PVR module is however, still very slow as compared with the parallel FDM simulation itself. For example the computation time taken for the volume visualization of $512\times256\times512$ model and the image resolution of $640\times480$ is about 1 s by parallel computing using 16 node (256CPU) of parallel processors, which is about ten times slower then the FDM simulation (about 0.1 s per time step). The improvements in the performance of the volume visualization on the Earth Simulator is an important subject of our current study.

### 3.3. Parallel Simulation of 2000 Tottori-ken Seibu Earthquake

A large ($M_J$7.3), inland earthquake occurred in Tottori, Japan, in 2000, which was the largest event since the destructive Kobe earthquake ($M_J$7.2) in 1995.

The ground motion from the large earthquake was well recorded at 521 stations of the nation-wide dense strong motion network across Japan (K-NET and KiK-net; Figure 1). The array stations were installed in the Japanese island just

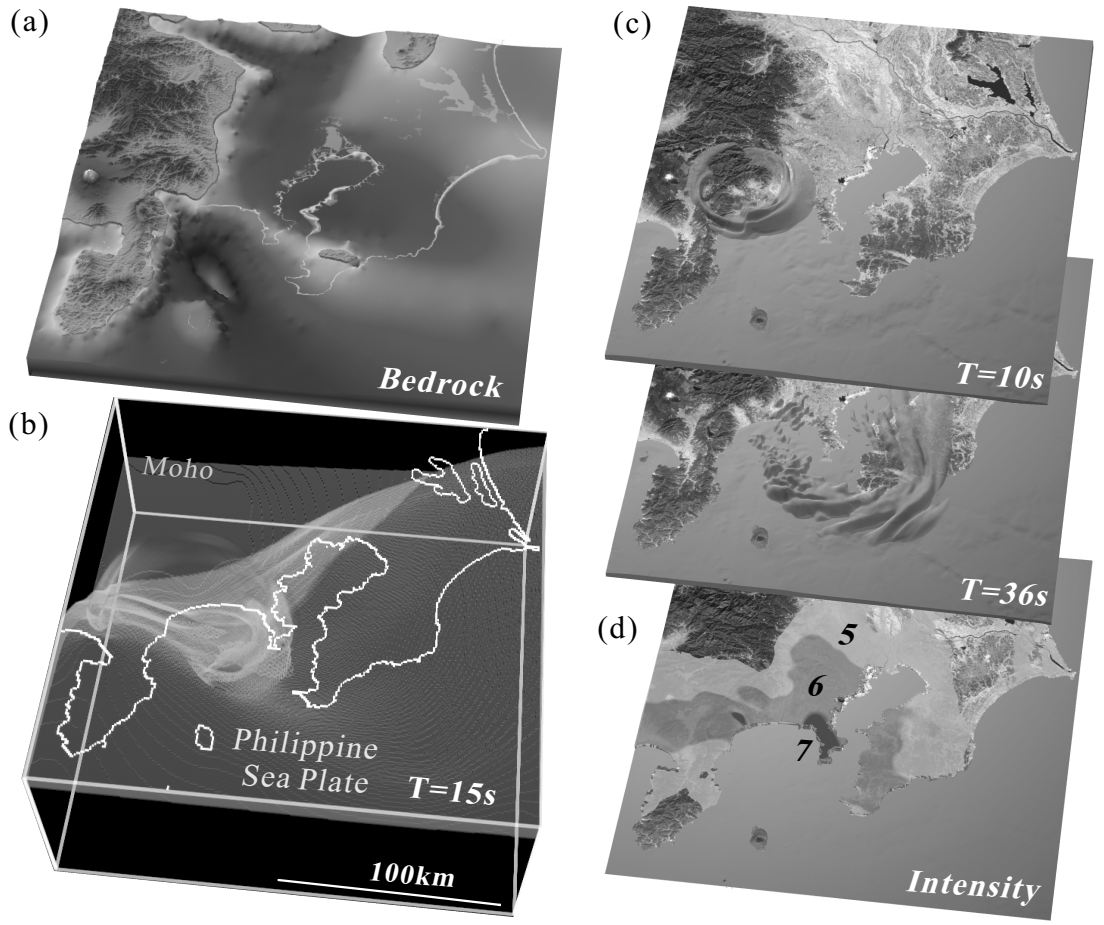


**Figure 4:** *(a) Structural model of sediment/bedrock interface beneath Tokyo. (b) Snapshot of seismic wave propagation radiating from the source (green area) on the Philippine-sea plate during the 1923 Kanto Earthquake, and (c) propagation of two large pulses on the surface. (d) Simulated intensity of ground motion from the earthquake. Color image is shown in last page.*

after the Kobe earthquake in order for mitigation of earthquake disaster by understanding the wave propagation and localized amplification characteristics at each site of island during large earthquakes.

We first demonstrates computer simulation of seismic wave propagation for the Tottori-ken Seibu earthquake in order to demonstrate the effectiveness of large-scale parallel simulation of seismic wave propagation by comparing with the observed ground motions in the dense seismic array. The simulation model represents a 820 km by 410 km area and extends to a depth of 128 km, which is discretized into elements with dimensions of 0.8 km by 0.8 km in the horizontal direction and 0.4 km in the vertical direction. The model is surrounding by 20-grid-points absorbing buffer zone [CKKR85] to eliminate artificial reflections.

The subsurface structure model of western Japan is constructed based on large number of datasets such as from reflection and refraction surveys and travel-time tomography studies. The 3D model includes lateral changes in the crust/mantle interface and depth of the Philippine-sea plate [Figure 3(a)]. The fault rupture history for the earthquake was derived by inversion using the K-NET and KiK-net records and teleseismic waveforms [YK00]. The source model is introduced in the simulation model by a set of point double-couple sources on the fault plane. The seismic source radiating seismic wave with maximum frequency of 1 Hz.

The 3D model is partitioned vertically into 32 subdomains of equal grid numbers, and each subdomain is assigned to the same number of nodes of the Earth Simulator. The parallel simulation used 100 Gbyte of memory and a wall-clock time of about 20 min in parallel computation using 32 nodes (256 CPUs) of processors.

Figure 3 shows a set of snapshot of seismic wavefield derived from the simulation. The shallow source of the earth-

quake radiated large shear (S) wave in the crust, which can be clearly seen in the first frame of the 3D wavefield [Figure 3(b)] as a four-lobe pattern of large S wave surrounding the source. As the time increase, the development of large amplitude surface waves (*LQ*) on the surface is clearly seen. The *LQ* wave propagation in western Japan at a relatively low wave speed of about 2.7 km/s, so it takes over two minute to propagate out from the island through Kyushu.

The observed ground motions by dense seismic array on a regional scale making it possible to confirm the effectiveness of the computer simulation very clearly. There is a good correlation between the observations [Figure 3(c)] and the simulation [Figure 3(d)], except for a slight underestimation of the amplitude of surface waves. This is due to the incompleteness of amplification effect in the shallow layer which can not include in the current simulation model with a relatively larger grid size (0.4 km). The effect of deep basin structures in major population centers can also be clearly seen as regions of significant amplification and extension of seismic waves.

The good match between the computer simulation and observation premising the application of the current model to infer the pattern of ground motions expecting for old and future earthquakes.

## 4. Ground motion from the 1923 Kanto Earthquake

The great 1923 Kanto earthquake ($M_J$7.9) was one of a most destructive earthquake in recent Japanese history, killing over 100,000 peoples around Tokyo and Yokohama cities. Most of the damage was considered to be attributed to the fire of wooden-frame houses just after the earthquake.

The Kanto earthquake occurred at the interface of the the subducting Philippine-sea plate beneath Kanto area. Long historical document indicating that this type of earthquake has repeatably been occurred beneath Tokyo at almost constant recurrent interval of about 200 years. Thus, the understanding of the fault rupture process and corresponding strong ground motions during the 1923 event is very interesting for understanding the potential damage from future earthquake scenario, and for the designing of emergency preparedness for next earthquake.

The fault mechanism of the 1923 earthquake was interpreted as two large slips (>6 m) over the fault of about 30×120 km. The fault rupture started beneath Miura peninsula and the rupture propagates to south east at a rupture speed of about 2.5 km/s [WS95]. The large slip on the source fault produced two large pulses dominating in frequencies about 0.2 to 0.5 Hz. Such a low-frequency ground motions of relatively longer wavelength can propagates longer distances from the source to the center of Tokyo with quite less attenuation than high-frequency seismic signals. Soft sediments of thickness larger than 4 km covering the basin of Tokyo amplified the long-period seismic wave significantly by resonance in the low wavespeed layer. Therefore, the ground motion damage from the earthquake is considered to be produced by complex mechanism resulting from the complicated fault rupture process on the source and dramatic amplification in heterogeneous structure along the propagation path and in shallow structure of Tokyo basin.

The strong ground motion during the earthquake was available by early record of seismic instrumentation in Tokyo, but unfortunately, most of them are clipped out by large (>30 mm) and long shaking lasting over several minutes. We therefore need to conducted computer simulation in order for recovering the strong ground motions that struck Tokyo in 1923.

The simulation model cover the zone of 204 km by 204 km by 100 km, which is discretized by a grid size of 0.2 km by 0.2 km by 0.1 km. The model includes heterogeneous crust and upper mantle structure and subducting Philippine-sea plate. We assigned at each grid points proper elastic parameters and anelastic attenuation coefficients for P and S waves to model such structure. Detail structural model for the Kanto basin has been studied extensively at many institutions such as university, national institute, and metropolitan government office in order for the mitigation of earthquake disasters. We used recent studies of [YY02] who compiled the large dataset from different institutions to prepare a suitable model for computer simulations. The model is constructed by three sedimentary layers with minimum S-wave velocity of 0.4 km/s embedded over a rigid bedrock with a S-wave velocity of 3.2 km/s. Maximum thickness of the sedimentary layer is about 4 km at the center of Tokyo bay [Figure 4(a)]. The seismic source model is derived from the analysis of teleseismic waveform [WS95], and the source radiates seismic waves at maximum frequency of 1 Hz.

Snapshots of seismic wave propagation derived from the simulation is shown in Figure 4, demonstrating how the strong ground motion was generating from the rupture propagation on the subducting Philippine-sea plate and from the amplification in heterogeneous structure in Tokyo basin. We find two large seismic pulses propagating in Tokyo with relatively longer wavelength of order of kilometers and at a relatively lower propagation speed less than 2 km/s.

The estimated seismic intensity of the Japanese 7 point scale is shown in Figure 4(d) illustrating significant ground motions for intensity greater than 6 covering the wide area above the hypocenter. The pattern of seismic intensity agree well with observations estimated by the damage rate of wooden-frame houses [MT02].

## 5. Source Depth Estimation for the 1855 Ansei Edo Earthquake

It is known that the Tokyo metropolitan city has ever suffered from significant damage with seismic intensity larger than 6

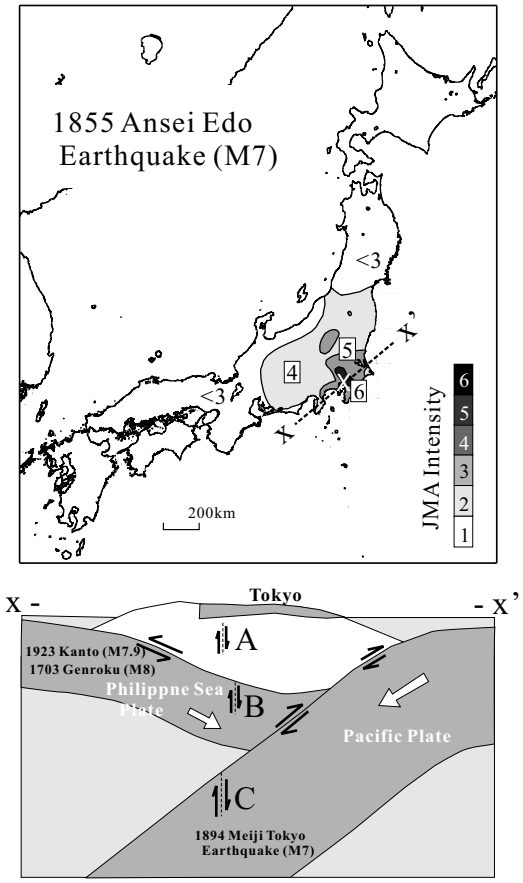


**Figure 5:** *(a) Pattern of seismic intensity during the 1855 Ansei Edo earthquake. (b) Schematic illustration of vertical cross section cutting Tokyo in x–x', and mechanism of major earthquakes which occur in the subsection zone of Tokyo.*

from three large earthquakes; Two of them were the 1923 Kanto earthquake (M7.9) and the 1703 Genroku earthquake (M8.4) both occurred at the top of the subducting Philippine-sea plate. The latter 1855 Ansei Edo earthquake (M7) is considered to be occurred in Tokyo bay, however, the source mechanism (depth) of the earthquake is still unknown.

Subsurface structure in Tokyo is very complicated due to the simultaneous subduction of the Philippine-sea plate and the Pacific plate beneath the continental North American plate. Large number of earthquakes of different mechanism occur by interactions among three plates and inside the three plates [Figure 5(b)]. Many researchers have been trying to find the source mechanism of the Ansei Edo earthquake by analyzing historical documents describing about the strong ground motions and damage during the earthquake.

Previous studies used the local intensity map in the area around Tokyo [HK01], so that the pattern of intensity distribution would be considerably affected by the site amplification effects of the shallow, localized structure rather than the source itself.

We therefore use the intensity distribution in regional scale, because major pattern of seismic intensity in regional distances would be affected by deep subsurface structure in the crust and upper mantle rather than the small-scale heterogeneities in the shallow structure beneath Tokyo.

The intensity pattern from the 1855 Ansei Edo earthquake is shown in Figure 5(a), demonstrating a peculiar distribution of intensity in regional scale. The intensity shows a rapid decay in intensity from 6 to 5 over the hypocenter, but the area of smaller intensity of 4 extending over wide area to several hundred kilometers in central Japan. The intensity shows almost isoseismic pattern, and so there is no clear extension of seismic contours to north as we usually seen such anomaly during deep earthquakes occurring at the subducting Pacific plate.

In order to find how the source depth change affect the regional seismic wavefield, and to find the best solution of the source model that explain the observed intensity during the Ansei Edo earthquake, we have conducted a set of simulations using three possible source models for source in (A) the crust (h=8 km), (B) the Philippine-sea plate (35 km) and (C) the Pacific plate (80 km).

The model of 3D simulation converse the area of 820 km by 410 km by 400 km, discretized by a grid of 0.4 km by 0.4 km by 0.2 km into 4 billion grid points. The seismic source is approximated by a double-couple point source, which imparts high-frequency seismic waves to 3 Hz. The parallel FDM simulation took computer memory of about 0.6 TByte and CPU time of 2 hours by parallel computing using 176 node (1408 CPU) of the Earth Simulator.

Figure 6(b) illustrating the snapshots of seismic wave propagation from the deep (h=80 km) plate event occurring at the Pacific plate, showing large amplitude P and S waves traveling in northern Japan. The subduction of the Pacific plate can transmit high-frequency seismic signals for longer distances without attenuation than propagating in surrounding mantle, so the resulting intensity from the earthquake shows anomalously large values along eastern seaboard of northern Japan [Figure 6(c)-(C)].

The simulated intensity from the intermediate depth (h=35 km) earthquake in the Philippine-sea plate shows almost isoseismic contours above the hypocenter with slight extension of contours along the plate. This resembles the pattern of intensity during the 1923 Kanto earthquake. Since the Philippine-sea plate seems to be too thin ($\sim$ 20 km) to keep seismic energy inside the plate, it should be difficult to produce anomalous extension of intensity contours along the subducting plate as we have seen for the thick ($\sim$ 80 km) Pacific plate.

On the other hand, the shallow (h=8 km) source produces

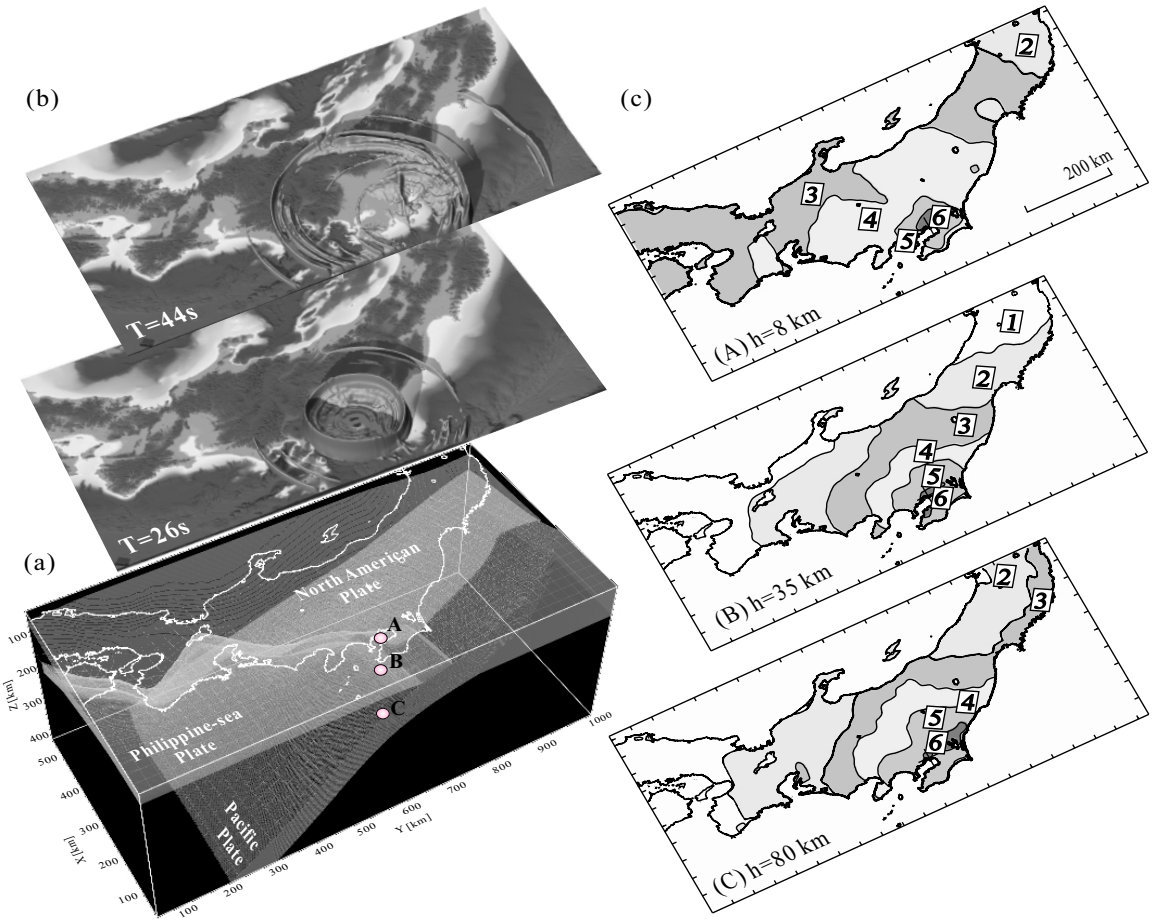


**Figure 6:** *(a) Structural model of central Japan used in the 3D simulation of seismic wave propagation, showing the configuration of crust and upper-mantle structure, Philippine-sea plate, and Pacific plate. (b) Snapshots of seismic wave propagation on the surface from a deep Pacific plate event [mark (C) in panel(a)] at time 26s and 44s from source initiation, and (c) simulated intensity pattern for three events at source depth (A) 8 km, (B) 35 km, and (C) 80 km.*

completely different intensity pattern from the other earthquakes occurring in the subducting plate, showing almost isoseismic pattern above the hypocenter. The intensity decays very quickly from 6 to 5 above the hypocenter, and then a gentle slope in attenuation extending over several hindered kilometers from the hypocenter [Figure 6(c)-(A)]. As compared with the simulated intensity patterns and observation, our preferable source model for the 1855 Ansei Edo earthquake is the shallow (h=8 km) event occurring in the crust. The simulated waveform shows that the lowered decay of seismic intensity arise due to the dominance of the multiple S-wave reflections in the crust as is well known as the 'Lg wave'. Such a crustally trapped Lg wave is often recognized in the regional seismographs in Japan at distances over 150 km from epicenter as a largest S waves during shallow crustal earthquakes [FK01].

## 6. Conclusions

The character of the seismic wavefield is controlled by the radiation of seismic waves imposed by complex source rupture history on the fault and the variation of subsurface structure along the wave propagation paths. For the prediction of strong motions for future events, we need a good understanding of the details of the 3D structure and seismic wavefield imposed by such heterogeneities.

We can hope to recover such information by combination between large number of seismic observations and high-resolution computer simulations to compliment each other with a suitable visualization techniques for 3D seismic wavefield.

Recent developments of dense nation-wide network (K-NET and KiK-net) and large-scale parallel computing envi-

ronment (the Earth Simulator) made it possible to such collaborative studies. The developments in efficient visualization tool for seismic wavefield is still increasing in demand.

We have shown by examples of computer simulation of seismic wave propagation and comparison between observations for recent and historical damaging earthquakes in Japan that the simulation of the seismic wave propagation is almost achieved a suitable level to demonstrating major pattern of strong ground motion characteristics during large earthquakes. Further improvements in the understanding of complex seismic wavefield and highly reliable computer simulations will depend on maintaining close link between seismology and computer visualization studies.

## 7. Acknowledgment

This study was suppurated by a joint research project with the Earth Simulator Center under the title “Numerical simulation of seismic wave propagation and strong ground motion in 3D heterogeneous media". Figures were drawn using the POV-Ray rendering software developed by C. Cason. Part of this study is suppurated by Special Project for Earthquake Disaster Mitigation in Urban Areas from Ministry of Education, Culture, Sports, Science and Technology. The K-NET and the KiK-net waveform data are available on the NIED website (http://www.bosai.go.jp). Supplemental MPEG movies of seismic wave propagation in Figures. 3, 4, and 6 can be viewed at the web site (http://www.eri.u-tokyo.ac.jp/furumura/EGPGV04/).

## References

[CFN03] CHEN L., FUJSIHIRO I., NAKAJIMA K.: Optimizing parallel performance of unstructured volume rendering for the earth simulator. *Parallel Computing 29* (2003), 355–371. 4

[CKKR85] CERJAN C., KOSLOFF K., KOSLOFF R., RESHEF M.: A nonreflecting boundary condition for discrete acoustic and elastic wave equation. *Geophysics 50* (1985), 705–708. 5

[FC04] FURUMURA T., CHEN L.: Large scale parallel simulation and visualization of 3D seismic wavefield using the Earth Simulator. *CMES (Submitted)* (2004). 3, 4

[FK01] FURUMURA T., KENNETT B.: Variations in regional phase propagation in the area around Japan. *Bull. Seism. Soc. Am. 91* (2001), 294–308. 8

[FKK03] FURUMURA T., KENNETT B., KOKETSU K.: Visualization of 3D wave propagation from the 2000 Tottori-ken Seibu, Japan Earthquake: Observation and numerical simulation. *Bull. Seism. Soc. Am. 93* (2003), 870–881. 3

[FKT98] FURUMURA T., KENNETT B., TAKENAKA H.: Parallel 3-D pseudospectral simulation of seismic wave propagation. *Geophysics 63* (1998), 279–288. 2

[FKW02] FURUMURA T., KOKETSU K., WEN K.-L.: Parallel PSM/FDM hybrid simulation of ground motions from the 1999 Chi-Chi, taiwan, earthquake. *Pure and Applied Geophysics 159* (2002), 21330–2146. 2

[HK01] HIKITA T., KUDO K.: Estimation of source parameters and strong ground motions during the 1855 Ansei-Edo earthquake by the empirical Green function method. *J. Struct. Eng. AIJ* (2001), 63–70. 7

[Lev88] LEVOY M.: Display of surfaces from volume data. *IEEE CG&A 8* (1988), 29–37. 3

[MT02] MOROI T., TAKEMURA M.: Re-evaluation on the damages statistics of wooden houses for the 1923 Kanto earthquake and its seismic intensity distribution in and around Southern Kanto district. *J. Seismological Eng. Japan* (2002), 35–71. 6

[RKEH88] RESHEF M., KOSLOFF D., EDWARDS M., HSIUNG C.: Three dimensional acoustic modeling by the Fourier method. *Geophysics 53* (1988), 1175–1183. 2

[SW90] SMITH W., WESSEL P.: Griding with continuous curvature splines in tension. *Geophysics 55* (1990), 293–305. 3

[WS95] WALD D., SOMERVILLE P.: Variable-slip rupture model of the great 1923 Kanto, Japan, earthquake: Geodetic and body-waveform analysis. *Bull Seism. Soc. Am. 85* (1995), 159–177. 6

[YK00] YAGI Y., KIKUCHI M.: Source rupture process of the tottori-ken seibu earthquake of Oct. 6, 2000, (Mjma 7.3) by using joint inversion of far-field and near-field waveform. *Abst. Seism. Soc. Japan 2000 Fall Meet.* (2000), T04. 5

[YY02] YAMANAKA H., YAMADA N.: Estimation of 3d s-wave velocity model of deep sedimentary layers in Kanto plain, Japan, using microtremor array measurements. *Butsuri-Tansa 55* (2002), 53–65. 6

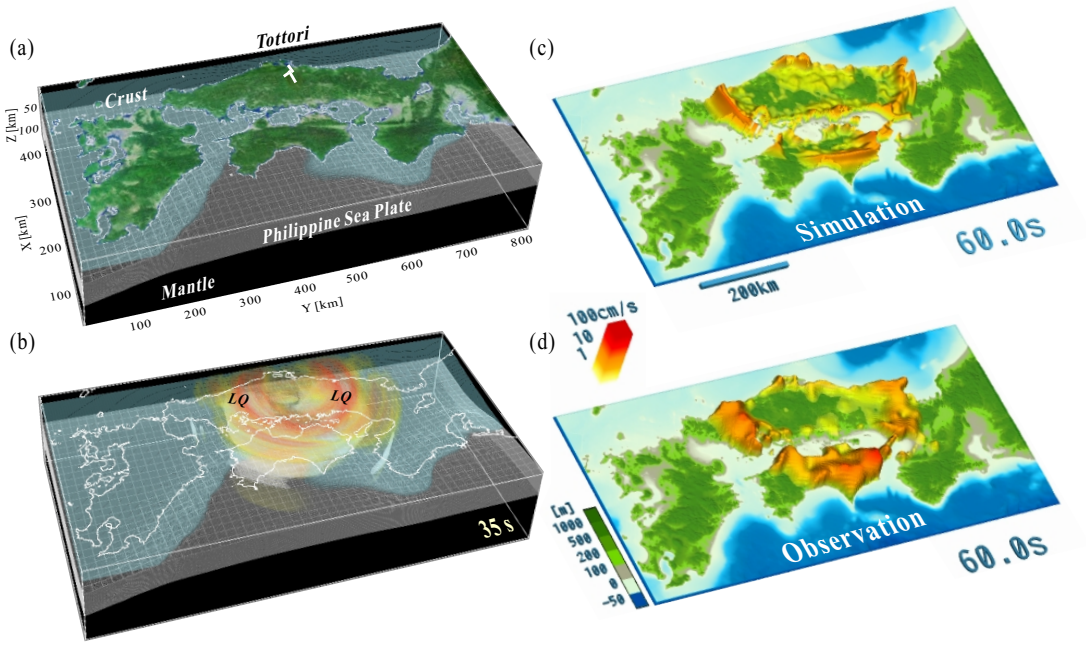


**Figure 3:** *(a) Structural model of western Japan used in the 3D simulation of seismic waves, showing the configuration of crust and upper-mantle structure and the Philippine-sea Plate. Snapshot of (b) seismic wave propagation from the source after 35s from the source initiation, and comparison between the wavefield at 60s for the (c) simulation result with (d) observation by dense seismic array.*

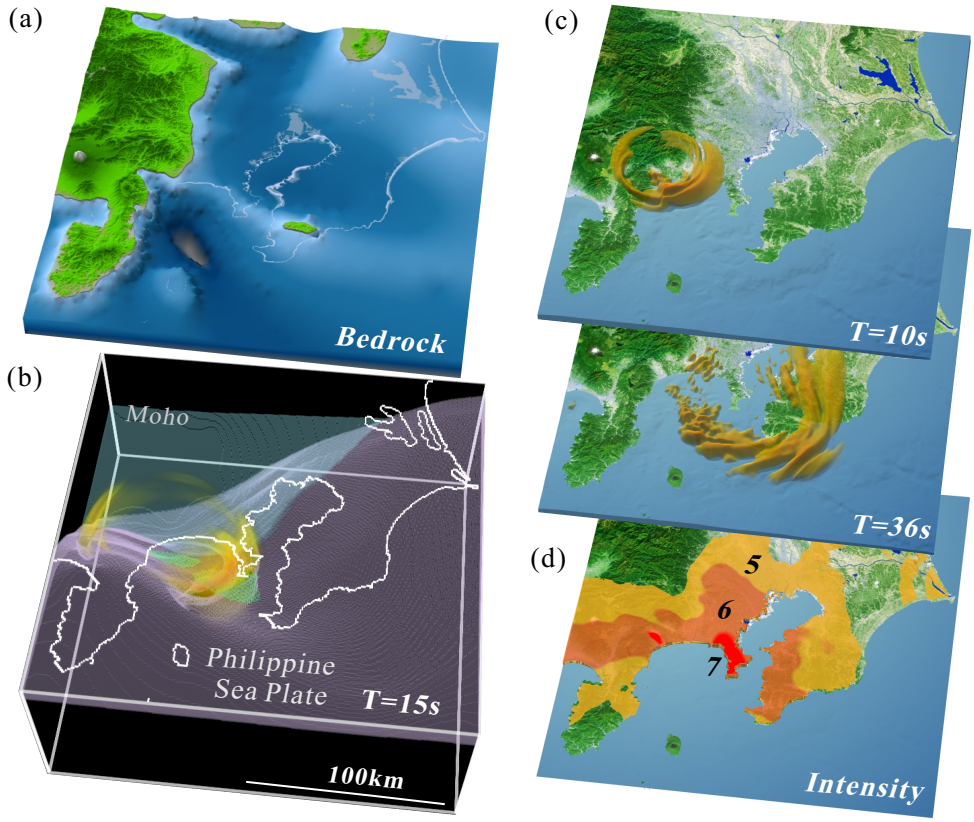


**Figure 4:** *(a) Structural model of sediment/bedrock interface beneath Tokyo. (b) Snapshot of seismic wave propagation radiating from the source (green area) on the Philippine-sea plate during the 1923 Kanto Earthquake, and (c) propagation of two large pulses on the surface. (d) Simulated intensity of ground motion from the earthquake.*